Ab Initio Study of Hydrogen Bonding Interaction and Photoinduced Electron Transfer between 4-nitroquinoline-1-oxide and Tryptophan

JI-FENG LIU, XIANG-YUAN LI, QUAN ZHU

College of Chemical Engineering, Sichuan University, Chengdu 610065, China

Received 30 June 2003; accepted 10 November 2003

DOI 10.1002/qua.20005

ABSTRACT: In the present article, the electronic structure of 4-nitroquinoline-1-oxide (4NQO) has been theoretically investigated at the level of HFSCF/6-31G**. Conformation of monomeric 4NQO has been found to be the most stable when the nitro group twists from the quinoline plane by about 24°. The absorption spectra of the twisted 4NQO have been calculated by using complete active space self-consistent field method. The hydrogen bonded complexes of 4NQO and tryptophan have been intensively studied. The absorption spectra of the most stable complex have been calculated to investigate the photoinduced electron transfer between 4NQO and tryptophan. The first and second excited singlet states are found to be charge-separated. Population analysis shows that the low-lying triplet states are charge-separated as well, except for the lowest one that presents the characters of a locally excited state. A solvent effect on transition energies has been considered based on the Ooshika–Lippert–Martaga equation. Theoretical study shows that the optical excitation can lead to charge separation in the 4NQO–tryptophan complex. Int J Quantum Chem 98: 33–43, 2004

Key words: absorption spectrum; charge separation; electron transfer; solvation correction

Introduction

Tryptophan radical ($Trp^{\bullet}$) and radical cation ($TrpH^{+}$) have important biological effects, including oxidative damage, carcinogenicity, and aging [1, 2]. Thus, it is very important to understand the mechanism of the oxidation of TrpH. In recent years, theoretical efforts have been made to understand the mechanism of the oxidation of TrpH by investigating its electronic structure as well as chromophore [1, 3, 4]. Experimental observations showed that the electron transfer is a crucial step in a series of processes that occur in biological systems. It is generally believed that TrpH is first oxidized to $TrpH^{+}$ or $Trp^{\bullet}$ after deprotonation; the electron transfer process then occurs from $TrpH^{+}$

Correspondence to: X.-Y. Li; e-mail: xyli@scu.edu.cn

Contract grant sponsors: National Natural Science Foundation of China; Trans-Century Training Program Foundation for the Talents by the Education Ministry of China.

or $Trp^{\bullet}$ to electron acceptor, such as the tyrosine or tyrosine radical anion. The oxidation of TrpH can be achieved by photolysis through direct ultraviolet (UV) light irradiation [5–7] or thermodynamic reactions with pulse radiolytically generated radicals, such as Br_2^-, $(SCN)_2^-$, and $N_3^{\bullet}$ [8–11]. Recently, another method of oxidizing the neutral TrpH into $TrpH^+$ has been explored. Some neutral molecules, such as 4-nitroquinoline-1-oxide (4NQO) and its derivatives, can oxidize TrpH through photon absorption [12, 13]. The triplet 4NQO was claimed to form an excited complex with TrpH, followed by the electron transfer process, associated with protonation of 4NQO and deprotonation of TrpH [13]. However, in our view, there may be a directly photoinduced electron-transfer process between 4NQO and TrpH. The present study clarifies our assumptions of direct photoinduced electron transfer through theoretical calculations.

4NQO is a typical carcinogenic substance [12, 14–19]. It has been established that 4NQO has the ability to bind to DNA via charge-transfer interaction in aqueous solution [12, 14–17]. In fact, experimental investigations on the biological effects of 4NQO have been carried out since the early twentieth century. Photochemical reactions of 4NQO with amino acids, DNA, and related compounds in aqueous solutions have been studied using a laser flash photolysis technique. Under irradiation with a 355-nm light pulse, the triplet state of 4NQO is formed, characterized by an absorption spectrum with a maximum at 410 and 590 nm [12–14, 20–24]. The electronic structure and electron spectra of 4NQO and its radical ions have been studied both experimentally and theoretically by several groups [21, 23–27].

In the present article, the authors focus on the interaction between TrpH and 4NQO and on the mechanism of electron transfer in peptide induced by 4NQO through photon absorption. First, the geometry and the absorption spectra of isolated 4NQO are investigated. Secondly, the hydrogen-bonding interaction between 4NQO and TrpH is studied and the stable complex of them, denoted [TrpH ⋯ 4NQO], is optimized. Finally, the excited states of [TrpH ⋯ 4NQO] are investigated.

Theoretical Methods

All calculations are performed using the HONDO99 program [28]. The ground states and excited states of 4NQO and its hydrogen bonding complex with TrpH are investigated by employing the complete active space self-consistent field (CASSCF) method. The molecular orbitals (MO) from RHFSCF have been used to induce the CASSCF calculations.

To make the calculated absorption spectra comparable to experimental results, the correction of solvent effect should be considered. The well-known Ooshika–Lippert–Martaga equation [29, 30] has been widely used in the solvent-shift correction of absorption spectrum. According to this theory, and applying Ooshika's theory to the case in which the solvent molecules surrounding the solute molecule are in the equilibrium configuration appropriate to the charge distribution of the ground state of solute molecule, one can obtain the solvation energy ΔE^m of the m state of the solute molecule. In the point-dipole approximation, without taking higher-order terms into account, the expression of ΔE^m can be simplified as follows:

$$\Delta E^m = -\frac{\boldsymbol{\mu}_g \cdot \boldsymbol{\mu}_m}{a_0^3}\left[\frac{2(\varepsilon-1)}{2\varepsilon+1} - \frac{2(n^2-1)}{2n^2+1}\right] - \frac{1}{2}\frac{2(n^2-1)}{2n^2+1}\frac{\boldsymbol{\mu}_m^2}{a_0^3} \quad (1)$$

where $\boldsymbol{\mu}_g$ and $\boldsymbol{\mu}_m$ are the dipole moments of the ground state and of the m state, a_0 is the radius of the spherical cavity, and ε and n the static dielectric constant and the refractive index of the medium. In Eq. (1), the first term on the right-hand side represents the interaction energy between $\boldsymbol{\mu}_m$ and the orientational component of the reaction field, whereas the second term accounts for the contribution due to the electronic polarization of the medium. When the solvation energies of the ground state and the excited Franck–Condon state are represented as ΔE_e^g and ΔE_f^e, respectively, the solvation shift of absorption spectrum is given below [29]:

$$h\Delta\nu_a = \Delta E_f^e - \Delta E_e^g = \frac{2(\varepsilon-1)}{2\varepsilon+1}\frac{\boldsymbol{\mu}_g^2 - \boldsymbol{\mu}_g\cdot\boldsymbol{\mu}_e}{a_0^3} - \frac{(n^2-1)}{2n^2+1}\frac{(\boldsymbol{\mu}_e-\boldsymbol{\mu}_g)^2}{a_0^3} \quad (2)$$

Thus, the transition energy from the equilibrium ground state to the excited Franck-Condon state in solution can be expressed as

$$\Delta E_{\text{solu}} = \Delta E_{\text{gas}} + h\Delta\nu_a = \Delta E_{\text{gas}} + \left[\frac{2(\varepsilon-1)}{2\varepsilon+1}\frac{\boldsymbol{\mu}_g^2 - \boldsymbol{\mu}_g\cdot\boldsymbol{\mu}_e}{a_0^3} - \frac{(n^2-1)}{2n^2+1}\frac{(\boldsymbol{\mu}_e-\boldsymbol{\mu}_g)^2}{a_0^3}\right] \quad (3)$$

where ΔE_{gas} is the transition energy of gas phase. The radius of the solvent cavity used in the equa-

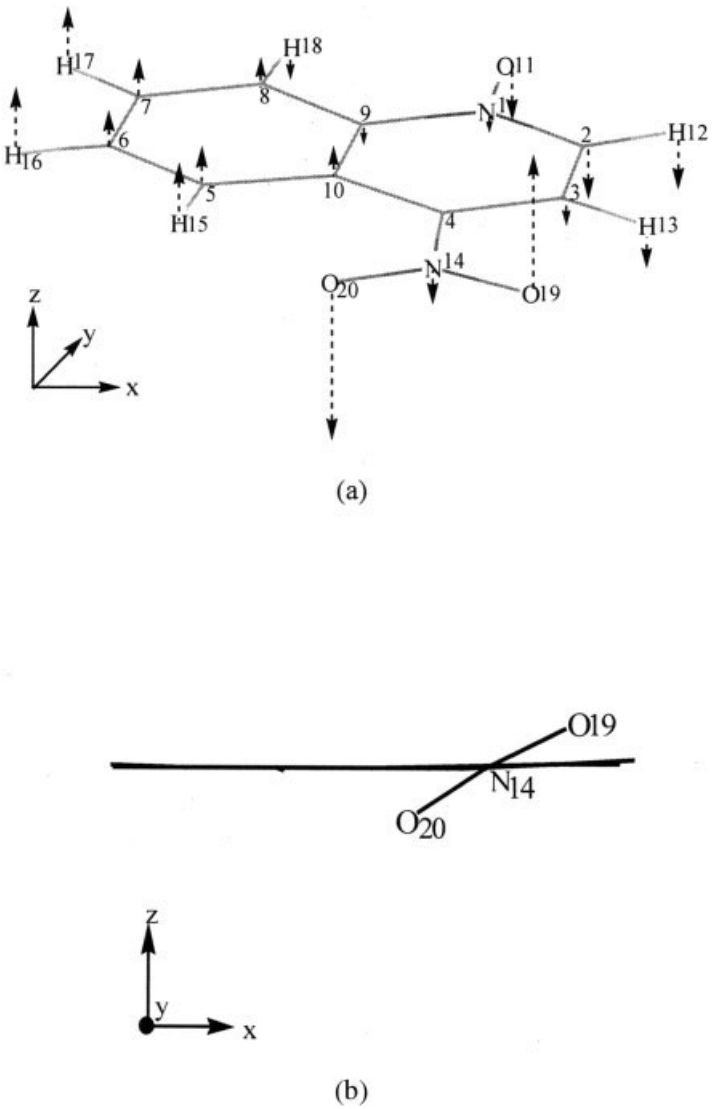

FIGURE 1. Schematic illustrations of planar 4NQO (a) and twisted 4NQO (b). Vibrational modes of the imaginary frequency in planar 4NQO are also shown in (a).

tions above is also an important variable, but it is difficult to determine. It was reported that the electronic isodensity method can yield relatively better results [31, 32]. In this method, the molecular volume of solute is defined as the volume inside a contour of 0.001 electrons/Bohr^3 density.

Results and Discussion

ABSORPTION SPECTRA OF 4NQO

At the HFSCF/6-31G** level, a planar conformation of 4NQO is optimized first, with a total energy of −677.59708 atomic units (a.u.). Frequency analysis shows that this planar conformation is not an energy minimum geometry, as an imaginary frequency arises mainly from the vibrational tendency along the axis linking O19 and O20 atoms, as shown in Figure 1(a). To obtain the stable geometry of 4NQO, geometry optimization is performed at the same basis level, with the starting geometry in which the nitro group twists from the quinoline plane by about 45°. No imaginary frequency is found according to frequency analysis. This means that the twisted geometry obtained after optimization corresponds to the energy minima. The nitro group possesses a twisted angle within the range of 24°–25°. This feature of the twisted angle was re-

TABLE I

Relative energies, dipole moments, and net charges on N and O atoms for different states of 4NQO.*

States	E_{re}	D_x	D_y	D_z	P_{N1}	P_{O11}	P_{N14}	P_{O19}	P_{O20}
S_0[a]	0	−0.529	0.142	−0.061	−0.167	−0.527	+0.398	−0.396	−0.397
S_1	3.539	−1.167	−1.472	−0.046	−0.334	−0.160	+0.409	−0.426	−0.424
S_2	4.570	−0.611	−1.466	−0.023	−0.247	−0.229	+0.406	−0.430	−0.401
T_1	1.738	−0.785	−0.743	−0.065	−0.387	−0.287	+0.377	−0.392	−0.410
T_2	3.504	−0.043	0.822	−0.034	−0.253	−0.510	+0.200	−0.242	−0.248

* Energy differences between two electronic states are given in eV, and dipole moments in a.u. (1 a.u. = 2.542 debyes).

[a] P_X represents the net charge on the X (X═N, O) atom.

[b] Total energy of S_0 is −677.70888 a.u. at the CASSCF/6-31G** level.

ported in the literature [23, 24]. The difference in total energy between the planar conformation and the twisted one of 4NQO is ~1.3 kJ · mol^{-1}, a very small value. Comparing the geometric parameters of the planar conformation with those of the twisted one, the differences of bond lengths are <0.004 Å, and those of the bond angles are <0.6°, except for the nitro group moiety. The values of dihedral angles for C3C4N14O19, C10C4N14O20, and C4N14O19O20 in twisted conformation are, respectively, 24.0°, 24.6°, and 178.5°.

To study the mechanism of photoinduced electron transfer between 4NQO and tryptophan, the electronic absorption spectra of 4NQO should be studied first. In this work, the six highest occupied molecular orbitals and the four lowest unoccupied molecular orbitals have been chosen as the active orbitals; thus, 12 active electrons are distributed in these 10 active molecular orbitals [hereafter abbreviated as CASSCF(12,10)]. The energy of the ground state has been calculated at the CASSCF(12,10)/6-31G** level based on the geometry optimized using the HF/6-31G** method. The Franck–Condon transitions of singlet excitations are then investigated based on the geometry of the ground state at the same level. The lowest triplet state is optimized at the CASSCF(12,10)/6-31G** level. A Franck–Condon transition of triplet excitations is studied based on the geometry of the lowest triplet state. Taking the total energy of the ground state S_0 as zero, the relative energies E_{re}, i.e., the energy differences between the specified states and the ground state, have been obtained and listed in Table I. The dipole components along three principal axes of 4NQO molecule, D_x, D_y, and D_z, as well as the net charges on N and O atoms have also been shown in Table I.

It can be seen in Table I that the net charge on O11 in the ground state is nearly twice that in the lowest triplet state, which implies that O11 is a better hydrogen acceptor in the ground state than in the lowest triplet state. And the net charge on O19 and O20 is approximately equal in both the ground state and the lowest triplet state. Furthermore, the net charge on O11 is larger than that on O19/O20. The results of the CASSCF calculation show that the lowest singlet excited state, S_1, is resulted from an $n \rightarrow \pi^*$ transition in which an electron jumps from an n-type occupied molecular orbital to a π-type unoccupied molecular orbital. The occupied molecular orbital is mainly contributed from the p_x and p_y atomic orbitals of O11. However, the unoccupied molecular orbital includes the combination of the p_z atomic orbitals of N1, C2, C4, C5, C6, C8, O11, N14, O19, and O20. Molecular analysis shows that the second excited singlet state S_2 is assigned to a $\pi \rightarrow \pi^*$ transition, in which one electron jumps from a π-type occupied molecular orbital which mainly contains the p_z atomic orbitals of N1, C2, C4, C5, C6, C8, and O11 to an unoccupied π-type molecular orbital, which is the same as that of the S_1 state.

To make the absorption transition energy calculation comparable to the experimental observation in aqueous solution, the solvent effect for the absorption spectra should be considered. The radius of solvent cavity has been estimated based on the geometry of ground state, and the recommended value of a_0 is 4.50 Å, which is obtained using the Gaussian 98 programs [33]. For aqueous solution, $\varepsilon = 78.5$, and $n^2 = 1.78$. Using Eq. (2), the solvation correction of the absorption spectrum can be obtained; the transition energy associated with the solvent effect is then calculated using Eq. (3). The solvation energy $h\Delta\nu_a$ and the transition energy calculated in the gas phase (ΔE_{gas}) of each available transition are presented in Table II.

TABLE II

Transition energies of 4NQO corrected by solvent effect.*

Transitions	ΔE_{gas}	$h\Delta\nu_a$	ΔE_{sol}	ΔE_{sol} (exp.)
$S_0 \rightarrow S_1$	3.539	−0.027	3.512	3.08 ~ 3.41,[a] 3.37[b]
$S_0 \rightarrow S_2$	4.570	−0.011	4.559	4.84 ~ 4.98,[a] 4.94[b]
$S_0 \rightarrow T_1$	1.738	−0.046	1.692	1.83[c]

* Energy in eV.
[a] Experimental value in cyclohexane, Ref. [21].
[b] Experimental value in water, Ref. [21].
[c] Experimental value of the triplet energy, Ref. [14].

From the results of our calculation, it can be seen that the differences between the transition energies of singlet excitation obtained in our calculation and in experiments are not more than 0.5 eV [21]. The energy difference between the ground state S_0 and the equilibrium lowest triplet state T_1 is calculated to be 1.738 eV in the gas phase and 1.692 eV after the solvation correction in water. The result of the theoretical calculation at the CASSCF(12,10)/6-31G** level is consistent with that by experimental measurement [14].

COMPLEX OF TRYPTOPHAN AND 4NQO

It was put forward by Seki et al. [12] that some proteins binding with DNA, RNA, and nucleic acid bases may participate in the process of carcinogenicity induced by chemicals. These kinds of proteins contain either TrpH or TyrOH residues, or both, such as lysozyme, ribonuclease, and histone. They are able to quench 4NQO at the same rate as a TrpH or TyrOH monomer, through electron transfer reactions, which means that the active site to 4NQO of these proteins is a TrpH residue or TyrOH residue. The electronic spectra of the aqueous solution of 4NQO and TrpH or TyrOH, or the proteins containing these two amino acid residues were investigated experimentally [12], but some phenomena remain unclear because of the limitations of the experiment condition. In this section, we focus on the interaction of 4NQO and TrpH. As the chemical and photochemical properties of tryptophan monomer were intensively investigated experimentally and theoretically in recent years [1, 4, 34, 35], we will not discuss the properties of tryptophan in the present article. The geometry of tryptophan in the complex with 4NQO has been fully optimized at the level of HFSCF/6-31G** based on the few available crystal structural parameters [36, 37].

HYDROGEN BONDING INTERACTION

As has been discussed above, the ground state of 4NQO has a greater tendency to form hydrogen-bonding complex with tryptophan than does the lowest triplet state of 4NQO. Thus, in this section, we will investigate the hydrogen bonding interaction between the ground state of 4NQO and tryptophan. As can be seen, both TrpH and 4NQO have conjugated huge π rings and, as mentioned earlier, the ground state of 4NQO has a strong tendency to form a hydrogen bond with a hydrogen donor. Thus, there are several types of encounter complexes for 4NQO and tryptophan due to the orientation of the N—H group attached to the heterocycle in tryptophan and that of the N-oxide group (N $\rightarrow$ O) in 4NQO, as well as the relative position of the two planes. Based on this point of view, we begin the geometry optimization with varied initial conformations, in which the two planes are parallel or coplanar. Six relative stable conformations of the complex [TrpH $\cdots$ 4NQO] have been obtained using full optimization at the HFSCF/6-31G level. Since only the hydrogen bonding interaction between the two moieties is of interest, we believe that optimization using Hartree Fock SCF method can give a good description for the complex. Frequency analysis shows that these conformations are energy minima. The six conformations are illustrated in Figure 2.

According to the results of our calculation, the six conformations of [TrpH $\cdots$ 4NQO] can be classified into two groups. In the first group, the hydrogen attached to the heterocyclic nitrogen atom of tryptophan approaches the N $\rightarrow$ O group of 4NQO and forms a relatively stronger hydrogen bond. It can be seen that conformations **I** and **II** are in this group. The other four conformations are in the second group, where the heterocyclic N—H group of tryptophan approaches the nitro group of 4NQO and forms a relative weaker hydrogen bond. Some parameters of hydrogen bonds formed in the six conformations are listed in Table III. The angle θ_{plane} formed by the two molecular planes has also been collected in Table III.

From calculation of the isolated species, the bond length of the heterocyclic N—H group in the TrpH monomer is 0.989 Å, its oscillation frequency is 3946.1 cm^{-1}, and the oscillation frequency of the O—H bond in the carboxylic acid group in the TrpH monomer is 3989.4 cm^{-1}. In all the conforma-

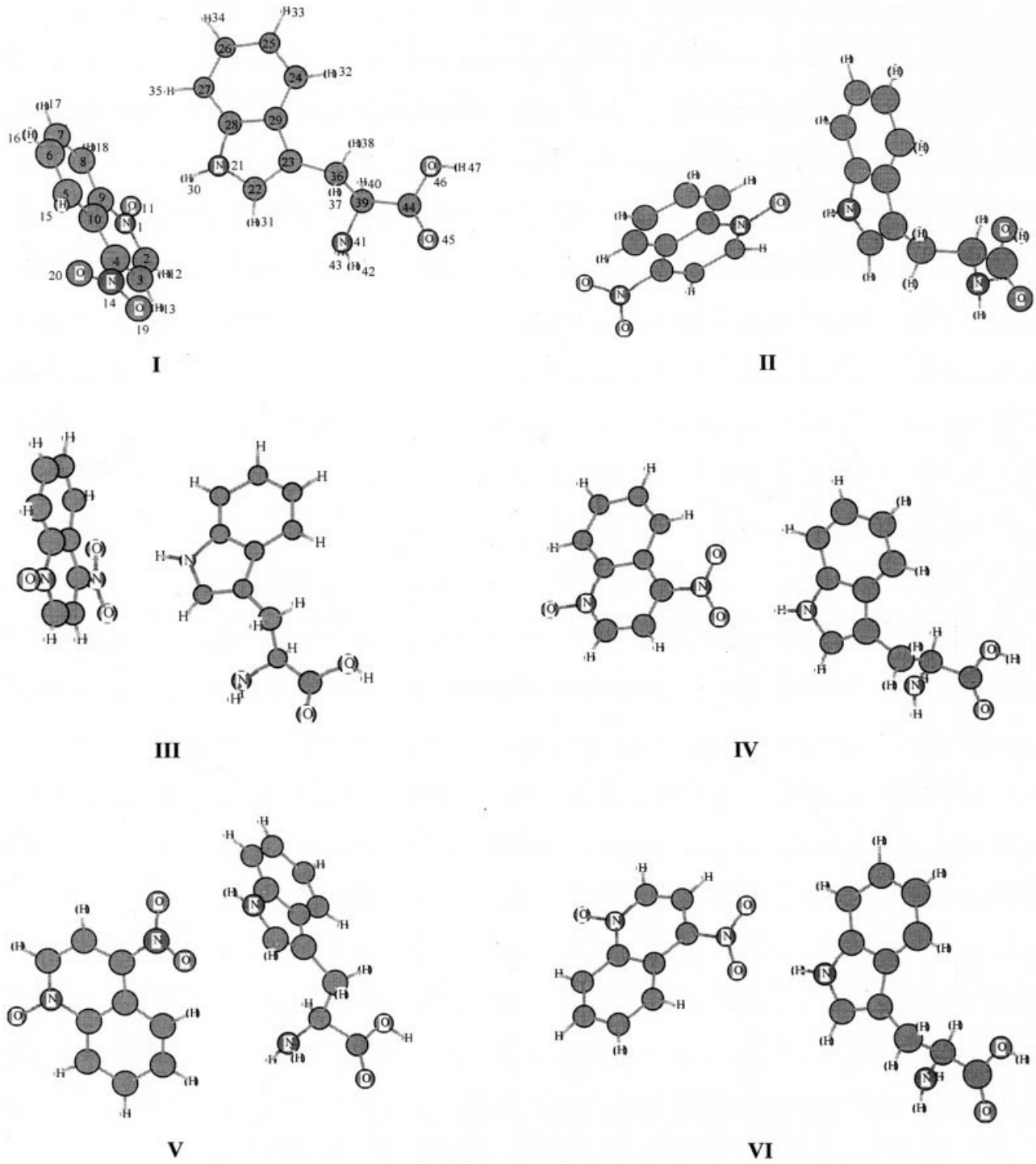

FIGURE 2. Schematic illustrations of several stable conformations of hydrogen bonded complex [TrpH · · · 4NQO]. All geometries have been optimized at the HFSCF/6-31G level.

tions, the bond length of the heterocyclic N—H group is 0.002–0.010 Å longer than that of the TrpH monomer, and the distance between the N and O atoms in N—H · · · O is within the range of 2.9–3.3 Å, suggesting the formation of a hydrogen bond. Therefore, we can conclude that all the conforma-

TABLE III

Structural parameters of the six conformations of [TrpH · · · 4NQO].

Conformations	$d_{N—H}$/Å[a]	$d_{N\cdots O}$/Å[b]	$\theta_{N—H\cdots O}$/(°)	$\nu_{N—H}$/cm^{-1} [c]	$\nu_{O—H}$/cm^{-1} [d]	θ_{plane}/(°)	ΔE_s/kJ · mol^{-1}
I	0.999	2.917	154.1	3778.5	3989.3	85.6	27.700
II	0.998	2.934	159.7	3793.8	3989.5	88.7	25.521
III	0.992	3.222	175.4	3910.2	3989.7	22.9	14.415
IV	0.992	3.214	172.7	3906.2	3989.7	10.8	14.467
V	0.991	3.207	141.4	3916.7	3989.3	84.6	11.946
VI	0.992	3.196	174.2	3901.6	3989.7	46.1	15.018

[a] Bond length of the heterocyclic N—H in TrpH moiety of [TrpH · · · 4NQO].
[b] Distance between N21 and O11/O19/O20.
[c] Oscillation frequency of the heterocyclic N—H in TrpH moiety.
[d] Oscillation frequency of O—H in carboxyl of TrpH moiety.

tions involve hydrogen bonding. For the hydrogen bonds are formed between heterocyclic N—H bond and O11 atom in conformation **I** and **II**, the oscillation frequency of the N—H bond in indole moiety of tryptophan shifts to the lower frequency by 167.5 cm^{-1} and 152.3 cm^{-1}, respectively, comparing with that of the tryptophan monomer. However, the frequency shifts of heterocyclic N—H bond in the other four conformations are ~45 cm^{-1}, much smaller than those of **I** and **II**. The oscillation frequency of the O—H bond in the carboxyl group of the complexes changes little compared with that of the tryptophan monomer. In addition, as mentioned previously in the present work, the electronic negativity of the N1–O11 group in 4NQO is larger than that of the N14–O19/O20 in the nitro group of 4NQO. Thus, it can be predicted that the hydrogen bond formed in the first group is stronger than that formed in the second group. In contrast, the stabilization energies of the conformations of [TrpH · · · 4NQO] can confirm this point of view.

The stabilization energies of the six conformations of [TrpH · · · 4NQO] have been calculated with the basis set superposition error (BSSE) correction being considered, and the approach introduced by Boys and Bernardi has been employed. This method is also usually called "function counterpoise" or "ghost orbitals," or simply the Boys–Bernardi (BB) method [38]. In the scheme of the BB method, the interaction energy of two molecules (A and B) can be expressed as follows:

$$\Delta E^{BB} = E_{AB}(AB) - [E_{Aeq}(A) + E_{Beq}(B)] - [E_A(AB) + E_B(AB)] + [E_A(A) + E_B(B)] \quad (4)$$

where $E_{AB}(AB)$ is the total energy of the complex, $E_{Xeq}(X)$ (X = A or B) is the total energy of monomer X with equilibrium geometry but without extended basis sets, and $E_X(AB)$ and $E_X(X)$ are the total energy of monomer X based on the same geometry as that in the complex with and without extended basis sets. Accordingly, applying Eq. (4), the stabilization energy, which is equal to the inverse value of the interaction energy of [TrpH · · · 4NQO] has been calculated and is also presented in Table III.

It can be seen that the stabilization energies of the six conformations of [TrpH · · · 4NQO] are all <40 kJ · mol^{-1}, but >10 kJ · mol^{-1}, meaning that there exist hydrogen bonds in all the conformations listed. The stabilization energies of conformations **I** and **II** are calculated 27.7 kJ · mol^{-1} and 25.5 kJ · mol^{-1}, respectively; thus, they are strong hydrogen-bonded conformations of [TrpH · · · 4NQO]. The stabilization energies of the other conformations are within the range of 12–15 kJ · mol^{-1}, so the hydrogen bonds in these conformations are rather weak. Comparison between the stabilization energies of these conformations gives a sequence of stability among the six conformations, **I** > **II** > **VI** > **IV** > **III** > **V**. The stabilization energy of conformation **I** is the largest; therefore, conformation **I** is the most stable one of [TrpH · · · 4NQO]. Thus, the following studies are based on the structure of conformation **I**.

PHOTOINDUCED ELECTRON TRANSFER INTERACTION

The phenomenon of photoinduced electron transfer appears widely in biosystems. It was reported that a special wave peak appears at 420 nm in the difference spectra of mixtures of any one of the four deoxyribonucleosides/DNA and 4NQO versus free 4NQO. The special absorption bands

TABLE IV

Total energies and dipole moments of the ground and excited states of [TrpH · · · 4NQO].*

States	E_t	D_t	D_x	D_y	D_z
S_0	−1359.23745	1.593	−1.098	0.921	−0.695
S_1	−1359.13381	9.866	1.551	−9.382	2.630
S_2	−1359.12242	10.120	0.453	−9.247	4.086
T_1	−1359.17533	2.329	−1.751	−1.456	−0.487
T_2	−1359.13416	9.860	1.514	−9.367	2.682
T_3	−1359.12627	9.989	0.610	−9.133	3.999

* Energies in a.u.; dipole moments in a.u. (1 a.u. = 2.542 debyes).

might be caused by electron transfer interaction, and there is a kind of relationship between the special absorption and the carcinogenicity of 4NQO [17]. Similarly, it is possible that an electron-transfer interaction occurs in the complex of 4NQO and TrpH. Thus, the photoinduced electron transfer in the complex [TrpH · · · 4NQO] has been tested. The vertical transition absorption spectra has been investigated using CASSCF(12,10)/6-31G. We chose the highest six doubly occupied orbitals and the lowest four unoccupied orbitals as the active space for our calculation, and distributed 12 active electrons in these active orbitals. All the active orbitals are π-type. The total energies of the ground state S_0, the first excited singlet state S_1, and the first two triplet states T_1 and T_2 have been obtained and are shown in Table IV. The total dipole moments, as well as their components along x, y, and z axes, are also listed in Table IV.

From the orbital analysis, we have noted that the first and the second excited singlet states are both formed as a result of the transition of one electron from the TrpH moiety to the 4NQO moiety. The total dipole moments of S_1 and S_2 are very large: 25.1 debyes for S_1 and 25.7 debyes for S_2. From the Mulliken population analysis of S_1 and S_2 states, it can be obtained that the net charge distributed on the 4NQO moiety is −0.913, and that on the TrpH moiety is +0.913 for the S_1 state. For the S_2 state, the net charge distributed on the 4NQO moiety is −0.916, and that distributed on the TrpH moiety is +0.916. Both S_1 and S_2 can be treated as charge-separated states. The net charge distributions on heavy atoms of different excited singlet states, as well as that of the ground state, are shown in Figure 3(a). The theoretical results show that the photoexcitation can directly lead to a charge separation in complex. The data in parentheses in Figure 3 are the bond indices [39, 40] of O · · · H and N—H of different electronic states, which show that the interaction of O11 and H30 becomes stronger and that of N21 and H30 becomes weaker in excited states except the lowest triplet state.

The net charge distributions of triplet states are shown in Figure 3(b). For the lowest triplet state T_1, the total net charges on 4NQO and TrpH moieties are almost zero. It can be safely concluded that the lowest triplet state is a charge-balanced state. Analysis of the molecular orbital components and of the corresponding coefficients of atomic orbitals reveals a feature of local excitation. The two unpaired electrons are located in the 4NQO moiety of the complex [TrpH · · · 4NQO]. The energy difference between the ground state and the lowest triplet state coincides with that of the 4NQO monomer, providing further evidence for the prediction of local excitation. Both the net charge distribution and the orbital analysis show that the second triplet state, T_2, is a charge-separated state. The total net charge on the 4NQO moiety of the T_2 state is equal to −0.913, and that on the TrpH moiety is +0.913. The dipole moment of T_2 state goes up to a large value, 25.1 debyes, reflecting the charge separation of T_2. The theoretical investigation shows that the T_3 state is also charge-separated. The total net charge on 4NQO moiety is equal to −0.915, and that on the TrpH moiety is +0.915. In summary, the theoretical results show that the higher excited triplet states and singlet states of complex [TrpH · · · 4NQO] are charge-separated states, which are resulted from the electron transfer from the TrpH moiety to the 4NQO moiety.

The transition energies of excited states in the gas phase have been calculated directly according to the total energy difference of the excited state and the ground state. The solvent effects on charge

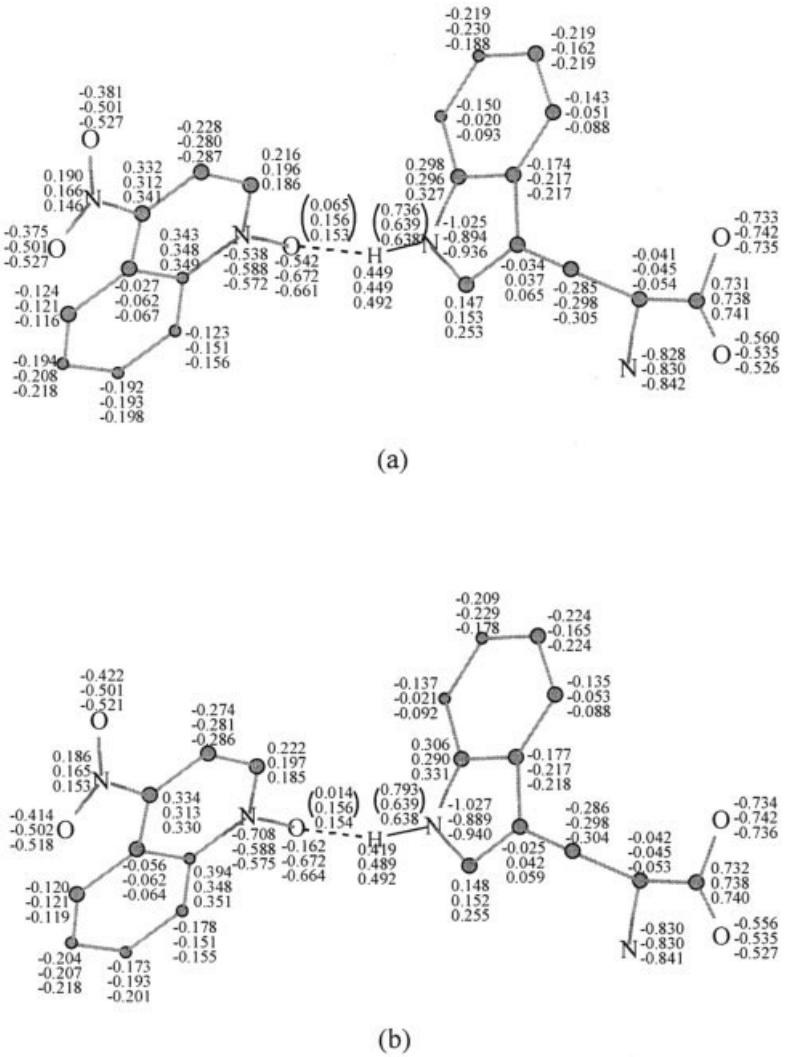

FIGURE 3. Net charge distributions of heavy atoms. (a) Data from top to bottom are for S_0, S_1, and S_2, respectively. (b) Data from top to bottom are for T_1, T_2, and T_3, respectively. Bond indices of O · · · H and N—H are given in parentheses.

separation states are remarkable. Therefore, using the method mentioned previously in this work, the solvation correction of the transition energy has been carried out. The radius of the spherical cavity, a_0, has been calculated 5.80 Å. When the aqueous solution is considered, the transition energies associated solvation correction have been calculated by employing Eq. (3). The Franck–Condon transition energies both in the gas phase and in aqueous solution have been presented in Table V accordingly.

The results of our calculation show that the solvent effect causes a red shift for the absorption spectra of charge-separated states. As shown in Table V, the transition energy from the ground state S_0 to the first singlet excited state S_1 is 2.705 eV in aqueous solution, corresponding to an absorption band at 458.4 nm. Several experimentally obtained spectra of 4NQO together with tryptophan, tyrosine, or proteins containing these two amino acids, or DNA in aqueous solution, show a strong and long-lived absorption at ~450 nm [12–14]. This absorption was assigned to the hydrogen adduct of 4NQO (4NQOH). However, our theoretical investigation of the photoinduced electron transfer in complex [TrpH · · · 4NQO] implies that the absorption band of the electron transfer transition between 4NQO and tryptophan is also near 450 nm. To

TABLE V

Solvation correction of transition energies of [TrpH · · · 4NQO].*

Transitions	ΔE_{gas}	$h\Delta\nu_a$	ΔE_{sol}
$S_0 \rightarrow S_1$	2.820	−0.115	2.705
$S_0 \rightarrow S_2$	3.130	−0.163	2.967
$S_0 \rightarrow T_1$	1.690	+0.011	1.701
$T_1 \rightarrow T_2$[a]	1.120	−0.381	0.739
$T_1 \rightarrow T_3$[a]	1.335	−0.382	0.953

* Transition energies in eV.

[a] The transition energies of $T_1 \rightarrow T_2$ and $T_1 \rightarrow T_3$ are corrected by taking the lowest triplet state T_1 as the initial state.

establish whether these two results are accidentally consistent requires more precise experimental and theoretical investigation. In addition, it was reported that a special wave peak appears at 420 nm in the difference spectra of free 4NQO versus the mixtures of 4NQO and any one of the four deoxyribonucleosides (dNs) or DNA. These special absorption bands might be caused by charge-transfer interactions, and there is a kind of relationship between the special absorption and the carcinogenicity of 4NQO [17]. Similarly, as demonstrated in our theoretical investigation, a charge-transfer interaction also exists in the 4NQO–TrpH complex. The transition energy from the ground state S_0 to the excited state S_2 is calculated to be 2.967 eV in aqueous solution, corresponding to an absorption peak at 417.9 nm. As depicted previously, the second excited singlet state is also a charge-separated state. Unfortunately, there is no experimental report on this charge-transfer absorption band in our system, or the mixtures composed from 4NQO and proteins containing TrpH residue. The special absorption spectrum of 4NQO solution, with and without DNA or any one of the four dNs, was obtained using higher concentration of the solution, which is 10^{-2} M with a 1:1 molar ratio [17]. However, as we know, the concentration of the solution of 4NQO and TrpH or proteins containing TrpH is in the range of 10^{-5}–10^{-3} M, and no special absorption spectrum appears in the difference spectra of 4NQO with and without TrpH. Thus, we can guess that the charge-transfer absorption spectrum was not detected because of the low concentration of the solution in previous experiments. We predict that a charge-transfer absorption spectrum of [TrpH · · · 4NQO] will appear if the concentration of the solution of the mixture and the molar ratio of 4NQO and TrpH is high enough.

Conclusion

The present article studies the structure and electronic absorption spectra of 4NQO. The absorption spectra have been calculated using both the CASSCF(12,10)/6-31G** and CASSCF(12,10)/6-31G methods. The results calculated after the solvation correction are consistent with experimentally achieved results. The first singlet transition $S_0 \rightarrow S_1$ of 4NQO is an $n \rightarrow \pi^*$ transition according to our theoretical calculations and analysis. The complex composed of 4NQO and TrpH has been studied intensively. Conformation optimization shows that the hydrogen bonded complexes of 4NQO and TrpH can be classified into two types: the strong hydrogen bonded complex with a stabilization energy of >25 kJ · mol^{-1}, and the weak hydrogen bonded complex with a stabilization energy within the range of 12–15 kJ · mol^{-1}. Investigation of the absorption spectra has been carried out based on the most stable conformation.

The first excited singlet state S_1 has been found to be a charge-separated state, and the first absorption peak is ~458 nm after solvation correction. We conclude that this absorption is caused by an electron transfer transition from the TrpH moiety to the 4NQO moiety. This absorption band is within the same range of wavelength that was assigned to the absorption of 4NQOH [12–14], but this needs more precise experimental and theoretical investigations to distinguish these two types of absorption. Furthermore, the results of our investigation show that the second excited singlet state S_2 is also a charge-separated state with an absorption peak at ~418 nm. This absorption band was assigned to the charge-transfer absorption in the hydrogen bonded complex of 4NQO and DNA. Our theoretical results indicate that the interaction between 4NQO and TrpH is similar to that between 4NQO and DNA [17]. Further experimental investigation is needed to verify this conclusion. The lowest triplet state of the complex is yielded from the localized excitation, which is attributed to the local electron transition in 4NQO moiety. The higher triplet states have been classified into charge-separated states, based on analysis of the charge distribution and calculation of dipole moments. According to theoretical investigation, we can predict that 4NQO and tryptophan form a hydrogen bonded complex in ground state

at first, and then one electron transfers from 4NQO to TrpH after light absorption, to form charge-separated excited singlet states. It can be predicted that the anion radical of 4NQO and the tryptophan cation radical can be formed, since the polar solvents can facilitate the separation of the ion pair. The intramolecular electron transfer in peptides involving the TrpH residue is possibly induced in this way. Further experimental evidence is needed to verify this hypothesis.

ACKNOWLEDGMENTS

The authors give special thanks to Professor Yu Shu-Qin and Dr. Sheng Zhen-Yu for their help in understanding the laser flash photolysis experiment.

References

1. Land, E. J.; Prütz, W. A. Int J Radiat Biol 1979, 36, 75–83.
2. Walden, S. E.; Wheeler, R. A. J Phys Chem 1996, 100, 1530–1535.
3. Lee, E.-J.; Medvedev, E. S.; Stuchebrukhov, A. A. J Phys Chem B 2000, 104, 6894–6902.
4. Tong, J.; Li, X.-Y. Chem Phys 2002, 284, 543–554.
5. Tan, D.; Reiter, R. J.; Chen, L.; Poeggeler, B.; Manchester, L. C.; Barlow-walden, L. R. Carcinogenesis 1994, 15, 215–218.
6. Bryant, F. D.; Grossweiner, L. I. J Phys Chem 1975, 79, 2711–2716.
7. Baugher, J. F.; Grossweiner, L. I. J Phys Chem 1977, 81, 1349–1354.
8. Feitelson, J.; Hayon, E. J Phys Chem 1973, 77, 10–15.
9. Redpath, J. L.; Santus, R.; Ovadia, J.; Grossweiner, L. I. Int J Radiat Biol 1975, 27, 201–204.
10. Posener, M. L.; Adams, G. E.; Wardman, P.; Cundall, R. B. J Chem Soc Faraday Trans 1 1976, 72, 2231–2239.
11. Land, E. J.; Prütz, W. A. Int J Radiat Biol 1977, 32, 203–207.
12. Seki, H.; Takematsu, A.; Arai, S. J Phys Chem 1987, 91, 176–179.
13. Sheng, Z.-Y.; Song, Q.-H.; Gao, F.; Zhou, X.-G.; Li, J.; Dai, J.-H.; Sun, H.-H.; Li, Q.-X.; Yu, S.-Q.; Ma, X.-X. Res Chem Intermed 2000, 26, 715–725.
14. Kasama, K.; Takematsu, A.; Yamamoto, S.; Arai, S. J Phys Chem 1984, 88, 4918–4921.
15. Nakahara, W.; Fukuoka, F.; Sugimura, T. Gann 1957, 48, 129–137.
16. Nagata, C.; Kataoka, N.; Imamura, A.; Kawazoe, Y.; Chihara, G. Gann 1966, 57, 323–335.
17. Okano, T.; Uekama, K. Chem Pharm Bull 1967, 15, 1812–1815.
18. Kubota, T.; Yamakawa, M.; Mizuno, Y. Bull Chem Soc Jpn 1972, 45, 3282–3286.
19. Kurihara, T.; Ichimura, H.; Igaki, T.; Ohta, A. Chem Pharm Bull 1971, 19, 37–40.
20. Kubota, T.; Miyazaki, H. Chem Pharm Bull 1961, 9, 948–961.
21. Okano, T.; Goto, M.; Matsumoto, H.; Takadate, A. Chem Pharm Bull 1972, 20, 2551–2560.
22. Miyazaki, H.; Kubota, T.; Yamakawa, M. Bull Chem Soc Jpn 1972, 45, 780–785.
23. Yamakawa, M.; Kubota, T.; Ezumi, K.; Mizuno, Y. Spectrochim Acta 1974, 30, 2103–2119.
24. Ezumi, K.; Kubota, T.; Miyazaki, H.; Yamakawa, M. J Phys Chem 1976, 80, 980–988.
25. Nelson, J. H.; Nathan, L. C.; Ragsdale, R. O. J Am Chem Soc 1968, 90, 5754–5757.
26. Kataoka, N.; Imamura, A.; Kawazoe, Y.; Chihara, G.; Nagata, C. Chem Pharm Bull 1966, 14, 1171–1178.
27. Kataoka, N.; Imamura, A.; Kawazoe, Y.; Chihara, G.; Nagata, C. Chem Pharm Bull 1966, 14, 897–902.
28. Dupuis, M.; Marpuez, A.; Davidson, E. R. "HONDO 99," 1999, based on HONDO 95.3, Dupuis, M.; Marpuez, A.; Davidson, E. R. Quantum Chemistry Program Exchange (QCPE); Indiana University: Bloomington, IN.
29. Mataga, N.; Kaifu, Y.; Masao, K. Bull Chem Soc Jpn 1956, 29, 465–471.
30. Ooshika, Y. J Phys Soc Jpn 1954, 9, 594–602.
31. Wiberg, K. B.; Keith, T. A.; Frisch, M. J.; Murcko, M. J Phys Chem 1995, 99, 9072–9079.
32. Foresman, J. B.; Keith, T. A.; Wiberg, K. B.; Snoonian, J.; Frisch, M. J. J Phys Chem 1996, 100, 16098–16104.
33. Gaussian 98, Revision A.9, Frisch, M. J.; Trucks, G. W.; Schlegel, H. B.; Scuseria, G. E.; Robb, M. A.; Cheeseman, J. R.; Zakrzewski, V. G.; Montgomery, J. A., Jr.; Stratmann, R. E.; Burant, J. C.; Dapprich, S.; Millam, J. M.; Daniels, A. D.; Kudin, K. N.; Strain, M. C.; Farkas, O.; Tomasi, J.; Barone, V.; Cossi, M.; Cammi, R.; Mennucci, B.; Pomelli, C.; Adamo, C.; Clifford, S.; Ochterski, J.; Petersson, G. A.; Ayala, P. Y.; Cui, Q.; Morokuma, K.; Malick, D. K.; Rabuck, A. D.; Raghavachari, K.; Foresman, J. B.; Cioslowski, J.; Ortiz, J. V.; Baboul, A. G.; Stefanov, B. B.; Liu, G.; Liashenko, A.; Piskorz, P.; Komaromi, I.; Gomperts, R.; Martin, R. L.; Fox, D. J.; Keith, T.; Al-Laham, M. A.; Peng, C. Y.; Nanayakkara, A.; Challacombe, M.; Gill, P. M. W.; Johnson, B.; Chen, W.; Wong, M. W.; Andres, J. L.; Gonzalez, C.; Head-Gordon, M.; Replogle, E. S.; Pople, J. A. Gaussian, Pittsburgh, PA, 1998.
34. Rizzo, T. R.; Park, Y. D.; Peteanu, L. A.; Levy, D. H. J Chem Phys 1986, 84, 2534–2541.
35. Rizzo, T. R.; Park, Y. D.; Levy, D. H. J Chem Phys 1986, 85, 6945–6951.
36. Bye, E.; Mostad, A.; Rømming, C. Acta Chem Scand 1973, 27, 471–484.
37. Hübschle, C. B.; Dittrich, B.; Luger, P. Acta Cryst 2002, C58, 540–542.
38. Boys, S. B.; Bernardi, F. Mol Phys 1970, 19, 553–577.
39. Armstrong, D. R.; Perkins, P. G.; Stewart, J. J. P. J Chem Soc Dalton 1973, 838–840.
40. Mayer, I. Chem Phys Lett 1983, 97, 270–274.